Localized Corrosion of Alloy 22 in the Potential Yucca Mountain Repository Environment

Xihua He and Todd Mintz

ABSTRACT

The U.S. Department of Energy (DOE) has indicated that it may use Alloy 22 as the waste package outer container material for the potential high-level waste repository at Yucca Mountain, Nevada. Additionally, a drip shield, made of Titanium Grade 7 and Titanium Grade 29, may extend the length of the emplacement drifts to enclose the top and sides of the emplaced waste package. Localized corrosion in the form of crevice corrosion could be one degradation process that may adversely affect the waste package performance. The main purpose of this paper is to summarize the work conducted previously to evaluate (i) the effects of environmental conditions relevant to the potential Yucca Mountain repository, metallurgical states (e.g., mill-annealed and welded plus solution annealed), and similar and dissimilar metal crevices on the crevice corrosion susceptibility of Alloy 22, and (ii) crevice corrosion propagation behavior by contacting to Alloy 22 or Titanium Grade 7. The results have shown that crevice corrosion susceptibility of Alloy 22 increased with increasing chloride concentration, temperature, and chloride-to-nitrate concentration ratios. Fabrication processes such as welding plus solution annealing also increased the localized corrosion susceptibility of Alloy 22. Compared to Alloy 22, Titanium Grade 7 appeared to be a more efficient cathode than Alloy 22 resulting in faster crevice corrosion propagation of Alloy 22.

INTRODUCTION

The DOE has indicated that it may use Alloy 22 (Ni–22Cr–13Mo–4Fe–3W) as the waste package outer container material for the potential high-level waste repository at Yucca Mountain, Nevada. The waste package may rest on an emplacement pallet made of Alloy 22. Additionally, a drip shield, made of Titanium Grade 7 (Ti–0.15 Pd) and Titanium Grade 29 [Ti–6Al–4V–ELI–0.10Ru (ELI stands for extra low interstitial referring to oxygen, nitrogen, hydrogen, and carbon)], may be extended over the length of the emplacement drifts to prevent seepage water and rockfall from contacting the waste packages. The drip shield bottom may be attached to Alloy 22 substructure to prevent direct contact between the drip shield and the invert support. In the absence of volcanic or seismic events, corrosion is expected to be the primary degradation process that may adversely affect the waste package performance. In the case of waste package breaching, radionuclides could be released and transported by groundwater.

Localized corrosion is one of the corrosion processes considered important in the potential degradation of the waste package outer container.[1] If localized corrosion occurs, it presumably would be in the form of crevice corrosion rather than pitting corrosion because of the high electrochemical potentials required to nucleate pits on an openly exposed surface in nickel-chromium-molybdenum alloys with high chromium and molybdenum (plus tungsten) content.[2] Metal-to-metal crevices may be formed by contact between the drip shield and the waste package outer container as a result of mechanical disruption (or failure) of the drip shield. Crevices may also be formed by metal-to-metal contact [e.g., (i) between the drip shield bottom and its Alloy 22 substructure, and (ii) between the outer container and the emplacement pallet] or metal-to-nonmetal contact by the deposition of mineral precipitates, corrosion products, dust, and contact with rocks. The chemistry of the water contacting the engineered barrier materials

depends on the seepage water composition and the evolution of the water chemistry and thermal hydrology within the emplacement drifts. Retention of aggressive solutions in occluded crevice areas at faying surfaces comprised of similar and dissimilar metals could lead to crevice corrosion of the engineered barrier system materials.

Crevice corrosion is commonly divided into three stages: initiation, propagation, and repassivation. The localized corrosion initiation abstraction in the U.S. Nuclear Regulatory Commission(NRC)/Center for Nuclear Waste Regulatory Analyses (CNWRA) Total-system Performance Assessment code is based on a critical potential model.[3] Crevice corrosion is considered possible if the corrosion potential (E_{corr}) of a metal in a given environment exceeds the repassivation potential for crevice corrosion (E_{rcrev}). In the NRC/CNWRA TPA code, repassivation of localized attack is assumed to occur only if the E_{corr} falls below the E_{rcrev}. On the other hand, if the E_{corr} of the container material is always above E_{rcrev}, localized attack is assumed to propagate without repassivation, and the localized corrosion penetration is computed as a function of time as

$$d = kt^n \qquad \text{(Eq. 1)}$$

where d is penetration depth; t is time; k is a rate constant dependent on environmental conditions; and the exponent n is a dimensionless constant.

In the NRC/CNWRA TPA code, n is assumed to be equal to 1 (i.e., once localized corrosion initiates, the localized attack is assumed to propagate linearly with time) and k is assumed to be 0.25 mm/y [9.8 mpy].

Numerous short-term tests have been conducted at NRC and CNWRA to measure the E_{corr} and the E_{rcrev} as a function of metallurgical and environmental conditions to assess the susceptibility of Alloy 22 to crevice corrosion using metal-to-polytetrafluoroethylene crevices.[4-7] Limited tests were conducted in NaCl solutions to understand the localized corrosion propagation behavior and the effects of similar and dissimilar metal crevices on crevice corrosion initiation and propagation. This paper summarizes the effects of environmental conditions (temperature, chloride concentration, and inhibitor concentration), metallurgical conditions (e.g., mill-annealed and welded plus solution annealed), and similar and dissimilar metal crevices on the crevice corrosion susceptibility of Alloy 22. In addition, the localized corrosion propagation by coupling to Alloy 22 or Titanium Grade 7 in NaCl solutions was also investigated.

MATERIALS AND METHODS

Repassivation potential, E_{rcrev}, measurements were conducted in a three-electrode glass test cell, which consisted of the crevice assembly as the working electrode shown in Figure 1(a), platinum as the counter electrode, and a saturated calomel reference electrode. The reference electrode was connected to the solution through a water-cooled Luggin probe with a porous glass tip to maintain the reference electrode at room temperature. Typically, the crevice is formed by sandwiching the Alloy 22 crevice specimen between formers made from a polymer or ceramic material wrapped with a polymer layer to fill the small voids created by the rough surface of the ceramic material. In addition to the mill-annealed Alloy 22 shown in Figure 1(a), welded plus solution annealed Alloy 22 specimens were used to evaluate the effect of fabrication processes on the corrosion performance of Alloy 22. Welded specimens were produced from a plate using gas tungsten arc welding with a U-groove joint geometry {25.4-mm

[1-in]-thick Alloy 22 with Heat 2277-3-3292 and Alloy 622 filler metal with Heat WN813 in Table 1}. The location of the weld is shown in Figure 1(a). Solution annealing of the as-welded specimens was performed at 1,125 °C [2,057 °F] for 20 minutes, followed by water quenching. Polytetrafluoroethylene is commonly used due to its chemical inertness and moderate rigidity. Upon torque, polytetrafluoroethylene deforms slightly and fills the small voids created by the surface roughness of the specimen, which results in a better occluded region and consistent crevice. For some tests used to study the effects of similar and dissimilar metal crevices, the crevice former was machined from metallic materials (Alloy 22 or Titanium Grade 7) as shown in Figure 1(b) and the crevice was assembled with the fixtures (bolts and nuts) machined from the same material as the crevice former.

The E_{rcrev} measurement was performed in a deaerated solution using cyclic potentiodynamic polarization with an intermediate potentiostatic hold.[6] The potential of the specimen was scanned from the open circuit potential to a higher potential at a scan rate of 0.1 mV/s, held at that potential for 8 hours, and then scanned down to -700 mV_{SCE} with a scan rate of 0.0167 mV/s until the current dropped below a specified value. The hold potential was limited to potentials below the onset of transpassive dissolution of Alloy 22. The E_{rcrev} is defined as the potential at which the current density drops below 2×10^{-6} A/cm^2 [1.9×10^{-3} A/ft^2] on the reverse scan of the polarization curve.[6]

Crevice corrosion initiation and propagation were evaluated by galvanically coupling the crevice specimen to either an Alloy 22 or a Titanium Grade 7 large plate. The test cell described in detail in previous publications [8,9] is shown schematically in Figure 2. The test cell with a total volume of approximately 350 mL [0.092 gal] was made of a glass cylinder compressed between polytetrafluoroethylene top and bottom lids. An Alloy 22 cylindrical specimen (Heat 2277-3-3266 in Table 1) with a diameter of 6.2 mm [0.24 in] was mounted perpendicularly through the center of the polytetrafluoroethylene bottom lid. The upper end of the Alloy 22 test specimen, with a surface area of approximately 1.5 cm^2 [0.23 in^2], was exposed to the test solution. A polytetrafluoroethylene bolt with a truncated cone-shaped tip was screwed through the center of the polytetrafluoroethylene top lid to press against the Alloy 22 flat surface, forming an artificial crevice. A torque of 0.35 N·m [3.1 in·lb] was applied to create a consistent crevice gap. A saturated calomel electrode was used as a reference electrode in all experiments. The Alloy 22 cylindrical specimen was galvanically coupled to an Alloy 22 (Heat 2277-1-3133 in Table 1) or Titanium Grade 7 plate (Heat CN2775 in Table 1) with a surface area of 60 cm^2 [9.3 in^2] using a potentiostat functioning as a zero-resistance ammeter. The Alloy 22 cylindrical specimen and plate and the Titanium Grade 7 plate were polished to a 600-grit finish, rinsed in deionized water, ultrasonically cleaned in acetone, and dried. The solution used in the test is 5 M NaCl, which is about half of the maximum chloride concentration expected in the potential repository due to seepage water evaporation. It is selected because consistent crevice corrosion initiation was observed previously during electrochemical tests.[6]

In this single-crevice assembly, crevice corrosion can occur as a result of the occluded environment created by the polytetrafluoroethylene bolt and the Alloy 22 cylindrical specimen surface. As crevice corrosion proceeds, the creviced Alloy 22 works as the anode and the plate as the cathode. With the setup used in this work, positive current corresponds to anodic current from the crevice specimen. The area ratio of the coupling Alloy 22 or Titanium Grade 7 plate to the cylindrical specimen was approximately 40:1, whereas the area ratio of the Alloy 22 exposed in solution to the crevice area was about 6 times that. The coupling potential and current densities were monitored throughout the tests. However, the measured current density

was not used for calculating the propagation rate, because the current flowing from the uncreviced area is not uniform across the crevice area. The crevice corrosion propagation behavior as a function of time was determined by performing tests for various durations after the initiation of crevice corrosion and subsequently examining the corroded specimens. The depth of the crevice corrosion penetrations was determined using a microscope following the method described in ASTM G46.[10]

RESULTS

Crevice Corrosion Initiation

Figure 3 summarizes the results of repassivation tests with mill-annealed and welded plus solution annealed Alloy 22 using polytetrafluoroethylene as crevice-forming material over a wide range of chloride concentrations at 95 °C [203 °F], along with the obtained E_{rcrev} values using metal (Alloy 22 or Titanium Grade 7) as the crevice-forming material in 0.5 M NaCl, 4 M NaCl, and 4 M $MgCl_2$ solutions at the same temperature. In Figure 3 the open symbols represent the tests where no crevice corrosion was observed and the closed symbols show where crevice corrosion was observed. For those tests where crevice corrosion did not occur, the E_{rcrev} has no physical meaning. The E_{rcrev} values were the hold potential during the measurement and are included in the figure to show the high resistance to crevice corrosion, but they were not used for comparison or any other data analysis. Overall, the E_{rcrev} values decreased with increasing chloride concentration suggesting the localized corrosion susceptibility increased with the increasing chloride concentration. Compared to mill-annealed Alloy 22, the welded-plus-solution annealed material has a lower E_{rcrev} value in similar chloride concentrations. The difference was more evident at chloride concentrations less than 0.5 M for the tests using polytetrafluoroethylene as crevice former. However, the E_{rcrev} values were very similar at higher chloride concentrations. Log-linear regression of the repassivation potential with chloride concentration resulted in the following equations:

Mill-annealed Alloy 22:

$$E_{rcrev} = -273\log_{10}[Cl^-] + 73.4 \quad \text{(Eq. 2)}$$

Welded plus solution annealed Alloy 22:

$$E_{rcrev} = -148\log_{10}[Cl^-] + 10.4 \quad \text{(Eq. 3)}$$

The regression lines shown in Figure 3 divide the plane into two regions: (i) above the line, the Alloy 22 material is susceptible to crevice corrosion and (ii) below the line, the Alloy 22 material is immune to crevice corrosion. The comparison of these two lines showed that the welded plus solution annealed Alloy 22 has a wider window of susceptibility to crevice corrosion than mill-annealed Alloy 22. Dunn, et al.[6] showed that the as-welded Alloy 22 and thermally aged Alloy 22 are also more susceptible to crevice corrosion than the mill-annealed Alloy 22.

For the repassivation tests using metal as crevice former in 0.5 M NaCl solution, no crevice corrosion was observed. In 4 M NaCl and 4 M $MgCl_2$ solutions, the E_{rcrev} values of metal-to-metal crevices where crevice corrosion was initiated were higher than those for metal-to-polytetrafluoroethylene crevices. The results suggest that the metal-to-metal crevices are less susceptible to localized corrosion than the metal-to-polytetrafluoroethylene crevices.

In the potential Yucca Mountain repository, anionic species such as nitrate, sulfate, carbonate, and bicarbonate are likely to be present in the groundwater or solutions produced by the salts in dust. Several studies[6] have shown that these species inhibit localized corrosion. Figure 4 shows the inhibiting effect of nitrate on the localized corrosion susceptibility of mill-annealed and thermally aged Alloy 22 in chloride solutions {thermally aged specimens were obtained by heating the specimen at 870 °C [1,598 °F] for 5 minutes}. Tests were performed in magnesium chloride solutions with the addition of nitrate at 80 and 110 °C [176 and 230 °F]. In 4 M $MgCl_2$ at 110 °C [230 °F], localized corrosion was observed in solutions with nitrate-to-chloride molar concentration ratios up to 0.1. At higher nitrate-to-chloride concentration ratios, no localized corrosion was observed. The nitrate to chloride molar concentration ratio necessary to inhibit localized corrosion at 80 °C [176 °F] was slightly lower. Similar results were obtained for thermally aged Alloy 22, but with higher nitrate-to-chloride ratios needed to inhibit localized corrosion. For example, at 110 °C [230 °F], localized corrosion was inhibited when the nitrate-to-chloride molar concentration ratio was 0.3. At 80 °C [176 °F], a nitrate-to-chloride ratio of 0.1 was sufficient to inhibit localized corrosion.

Crevice Corrosion Propagation Behavior of Alloy 22 Galvanically Coupled to Alloy 22 or Titanium Grade 7 in 5 M NaCl Plus 2 × 10^{-4} M $CuCl_2$ Solution at 95 °C [203 °F]

Galvanic coupling tests of Alloy 22 to Alloy 22 conducted by He and Dunn[8,9] showed that crevice corrosion of Alloy 22 was mitigated and had a strong tendency to repassivate, and the penetration rate tended to decrease significantly with time. Similar tests were conducted under the same conditions using a polytetrafluoroethylene crevice former with the addition of $CuCl_2$ solution in the single-crevice assembly test cell shown in Figure 2 to (i) investigate the crevice corrosion propagation behavior of Alloy 22 galvanically coupled to Titanium Grade 7 and (ii) compare it with previous results on crevice corrosion propagation of Alloy 22 galvanically coupled to Alloy 22 as reported by He and Dunn.[8,9] $CuCl_2$ is not present in the potential Yucca Mountain repository. It is added as an oxidant to increase the corrosion potential to initiate crevice corrosion.

Figure 5 shows the galvanic coupling current density and potential obtained from two tests. The current and potential in these two tests were very similar to those observed previously by coupling to an Alloy 22 plate.[8,9] After adding $CuCl_2$, crevice corrosion initiated. However, the current density decreased by 1–2 orders of magnitude after the initiation. Afterwards, the current density remained almost steady while crevice corrosion propagated. No repassivation was observed in these two tests. One of the tests was terminated after 39 days. The posttest examination of the specimen revealed crevice corrosion across the crevice area with a maximum penetration depth of 327 μm [12.9 mils].

In the other test, the polytetrafluoroethylene screw was backed up to open the crevice between the Alloy 22 specimen and the polytetrafluoroethylene screw after 108 days. Immediately after the crevice opened, the current density decreased and the corrosion potential increased to approximately 400 mV_{SCE}, indicating the repassivation of the crevice. This suggests that a tight crevice is required to maintain the composition of the critical solution necessary for crevice corrosion of Alloy 22. After 11 days of decrevicing, the current density increased, and the corrosion potential decreased, suggesting the reinitiation of crevice corrosion as shown in Figure 5. This test was terminated after 136 days. Posttest examination of the Alloy 22 specimen revealed that most of the corrosion occurred at the front surface of the Alloy 22 crevice region formed by the polytetrafluoroethylene screw. In addition, the side of the Alloy 22

cylinder contacting the bottom lid was slightly corroded, which could contribute to the crevice corrosion reinitiation observed in Figure 5. Figure 6 shows the posttest specimen with some corroded area covered by the residual corrosion products (black area) (location B in Figure 6). The maximum penetration depth was 460 μm [18.1 mils]. The corrosion products and the metal matrix exposed by corrosion were analyzed by scanning electron microscopy and energy dispersive x-rays to determine the alloying element dissolution during crevice corrosion. The compositions at locations A and B in the corroded area are shown in Table 2. Compared to the nominal composition of Alloy 22 in Table 1, the metal matrix in the corroded area has composition similar to the noncorroded Alloy 22, whereas the corrosion products are highly enriched in molybdenum and tungsten and depleted in nickel and chromium. Chloride was detected only in the corrosion products.

Ten tests were performed under these conditions. Figure 7 plots the maximum penetration depths (d_{max}) as a function of time from all the tests of Alloy 22 coupled to Titanium Grade 7 along with the penetration depths reported previously by coupling Alloy 22 to Alloy 22.[8,9] A fit of the experimental data to the exponential relationship yielded Eq. 4

$$d_{max} = 41.3t^{0.524} \qquad \text{(Eq. 4)}$$

where

t — time in days
d_{max} — maximum penetration depth in μm

The equation obtained previously by coupling Alloy 22 to Alloy 22 [8,9] is listed for comparison

$$d_{max} = 91.2t^{0.233} \qquad \text{(Eq. 5)}$$

The greater time exponent (0.524) suggests that crevice corrosion propagation of Alloy 22 is more efficient by coupling to Titanium Grade 7 in the same solution at the same temperature than by coupling to Alloy 22.

The anodic reaction in the crevice that leads to the Alloy 22 corrosion process is supported by the cathodic reaction occurring outside the crevice region. To understand the difference in the crevice corrosion propagation rate on Alloy 22 and Titanium Grade 7, limited cathodic reaction scans were performed at 95 °C [203 °F]. Figure 8(a) shows the cathodic polarization scans performed on Alloy 22 and Titanium Grade 7 in comparison with platinum from -0.35 to -1 V_{SCE} and backward at a scan rate of 5 mV/sec in aerated 5 M NaCl solution. The insert in the figure shows the comparison between Alloy 22 and Titanium Grade 7. Compared to the fast oxygen reduction reaction on platinum, the reaction on Alloy 22 and Titanium Grade 7 is suppressed. At potentials greater than -0.80 V_{SCE}, little difference was observed on Alloy 22 and Titanium Grade 7. However, at potentials less than -0.80 V_{SCE}, the oxygen reduction reaction was more efficient on Alloy 22 than on Titanium Grade 7. Similar polarization scans were performed on Alloy 22 and Titanium Grade 7 [shown in Figure 8(b)] from -0.10 to -1 V_{SCE} and backwards at a scan rate of 5 mV/sec in aerated 5 M NaCl plus 2×10^{-4} M $CuCl_2$ solution. The addition of 2×10^{-4} M $CuCl_2$ solution changed the cathodic reaction. One peak was seen on the reverse scan at -0.43 V_{SCE}, which could be associated with the oxidation of Cu^{+} to Cu^{2+}. The peak current density was higher on Titanium Grade 7 than on Alloy 22. In contrast to

Figure 8(a), the cathodic reaction at potentials less than $-0.80\ V_{SCE}$ was more efficient on Titanium Grade 7 than on Alloy 22.

DISCUSSION

In the potential Yucca Mountain high-level radioactive waste repository, the waste package outer container could form crevices by metal-to-metal or metal-to-nonmetal contacts. During fabrication, the waste package may be solution annealed to eliminate residual stresses. Therefore, both mill-annealed and welded plus solution annealed metallurgical conditions may be present in the Alloy 22 waste package outer container.[11,12] The potential use of Alloy 22 as the waste package outer container material may be based on the high resistance of the alloy to brittle fracture and accelerated degradation modes such as localized corrosion and stress corrosion cracking. However, formation of concentrated solutions in occluded crevice areas could lead to crevice corrosion of waste package materials. For Alloy 22, crevice corrosion occurs in solutions with high chloride-to-nitrate concentration ratios, with crevice corrosion susceptibility increasing with the increasing chloride concentration and temperature.

Interplay of Alloy 22 Passive Film Properties and Crevice Corrosion Resistance

The corrosion resistance of Alloy 22 has been attributed to a chromium-rich passive film formed on the surface of the alloy, which is stable over a range of environmental conditions. Metal alloys with stable oxide films offering corrosion resistance tend to be susceptible to crevice corrosion. This is especially true in chloride environments, where chloride can disturb the protective nature of these oxides.

For Ni-Cr-Mo alloys, the various alloying elements to the nickel-based alloy contribute to the corrosion resistance. The addition of chromium provides resistance against oxidizing environments while lowering the passivation potential and the passive dissolution current. Molybdenum provides resistance against reducing environments. The additions of both chromium and molybdenum are a strategy to provide protection against localized attack. Nickel, chromium, and molybdenum are thought to provide protection against chloride-induced stress corrosion cracking.

The one common feature in most of the proposed mechanisms for crevice corrosion initiation is that they all involve the breakdown of the surface film in one form or another. Many experimental studies[13-15] suggest a correlation between crevice corrosion resistance and a characteristic surface film. Tapping[13] utilized *ex-situ* scanning auger microscopy to examine the passive oxide film properties on iron-nickel-chromium-molybdenum alloys in corroded and noncorroded areas. There was no correlation of degradation with film thickness, but a compositional trend was observed for the elemental constituents chromium, molybdenum, and iron. An increase in oxide film protectiveness correlated with a decreasing iron concentration and an increasing molybdenum and chromium concentration. Hayes, et al.[15] examined the complementary roles of chromium and molybdenum in nickel alloy passivation. The study indicated that chromium plays a strong role in maintaining the passivity of the alloy, while molybdenum stabilizes the passive film after a localized breakdown event.

Lloyd, et al.[16] examined the behavior of both Alloy C276 (Ni-16Cr-16Mo-5Fe-4W) and Alloy 22 in acidic solutions. These acidic conditions are not expected in the potential repository setting but were considered in order to simulate the balance between the oxide film formation and

dissolution, expected over a longer period of time. The materials were examined in a 1.0 M NaCl + 0.1 M H_2SO_4 at a range of 25 to 85 °C [77 to 185 °F]. Despite the concept that Mo additions should lead to an increase in the resistance to passive film breakdown and localized corrosion initiation, localized corrosion of C276 initiated but not Alloy 22.

Lloyd, et al.[17] conducted an additional study which included C2000 (Ni-23Cr-16Mo-2Cu), C276, C4 (Ni-16Cr-16Mo-3Fe), Alloy 625 (Ni-21Cr-9Mo-5Fe), and Alloy 22. These alloys were passivated potentiostatically in deaerated 1 M NaCl + 0.1 M H_2SO_4 solution that was ramped from 25 to 85 °C [185 to 77 °F] during the test. With respect to crevice corrosion, the test indicated that C4 was most susceptible followed by Alloy 625 and then C276. No crevice corrosion initiated on either C22 or C2000. Similar to the results shown in the work by Lloyd, et al.,[16] the material with the lower chromium concentration was more susceptible to crevice corrosion. Following the same logic, C276 would have been expected to be susceptible, but it was not, and the main difference was the addition of tungsten to the alloy. Instead, Alloy 625 was found to have a higher susceptibility to crevice corrosion. Interestingly, Alloy 625 has a high chromium concentration but low molybdenum and no tungsten, which suggests that molybdenum does play a role in the reduced susceptibility for crevice corrosion. The next highest susceptible material was C276, which has less chromium. The results from these studies suggest that chromium, molybdenum, and tungsten play a role in reducing the susceptibility to crevice corrosion. The results suggest that molybdenum and tungsten play a common role. Additionally, MoO_4^{2-} in the outer region of the oxide may lead to a cation-selective character and discourage the incorporation of Cl^- into the passive film.

Macdonald[18] examined the role of molybdenum and other possible alloying elements using the point defect model. He suggested that the diffusivity of cation vacancies plays a critical role in the breakdown of the passive film. The alloying element role may involve the pairing between highly charged solute ions that are present in the barrier layer and the mobile cation vacancies. Macdonald argued that highly charged solutes such as Mo^{6+} and W^{6+} exert strong electrostatic interaction with mobile cation vacancies enhancing complexation and decreasing the diffusivity and concentration of mobile cation vacancies in the film.

Crevice Corrosion Propagation

Crevice corrosion could initiate by (i) the generation of an acidic environment in the crevice region that either depassivates the metal in the crevice and/or (ii) a potential drop in the crevice, shifting the dissolution of the metal from a passive to an active state.[19,20] For localized corrosion to propagate, the electrons produced from corrosion reactions in the anodic regions (crevices) should be consumed by the cathodic reactions. Therefore, the corrosion current produced by the anodic reaction must be balanced by the cathodic current for the sustained propagation of the localized corrosion front. If the cathodic reaction or the anodic reaction is a limiting factor due to mass transport, and the chemistry and geometry in the crevice are also limiting factors, the localized corrosion may become mitigated or even arrested.

It was previously reported that the penetration due to crevice corrosion of Alloy 22 was limited when coupled to Alloy 22 in a 5 M NaCl solution at 95 °C [203 °F] using polytetrafluoroethylene as the crevice former.[8,9] Figure 6 shows that Titanium Grade 7 appears to be a more efficient cathode than Alloy 22 (i.e., Alloy 22 coupled to Titanium Grade 7), leading to a faster crevice corrosion propagation than occurs when Titanium Grade 7 is coupled to Alloy 22 in the same solution at the same temperature. However, Figure 8(a) shows that at

potentials less than $-0.80\ V_{SCE}$, the oxygen reduction reaction was more efficient on Alloy 22 than on Titanium Grade 7. Figure 8(b) shows that the addition of 2×10^{-4} M $CuCl_2$ to NaCl solution changed the kinetics of the cathodic reaction. The higher peak at $-0.43\ V_{SCE}$ on Titanium Grade 7 in Figure 8(b) suggests that Cu^{2+} may participate in the cathodic reaction, and this reaction may be enhanced by the semiconductive oxide film on titanium. At potentials less than $-0.80\ V_{SCE}$, the cathodic reaction was more efficient on Titanium Grade 7 than on Alloy 22, which is contrary to that observed in NaCl solution without $CuCl_2$. The higher peak at $-0.43\ V_{SCE}$ and the higher cathodic reaction efficiency on Titanium Grade 7 than on Alloy 22 could account for the higher propagation rate shown in Figure 7. The faster crevice corrosion propagation by coupling to Titanium Grade 7 is presumably complicated by adding $CuCl_2$ to the NaCl solution. Alloy 22 and Titanium Grade 7 are covered with passive film, which strongly affects the cathodic reaction on the metal surface. Additional tests are needed to understand how the cathodic reactions change with the oxide film properties, considering the differences in the semiconductive properties of TiO_2 and the chromium-rich oxide film of Alloy 22.

For Alloy 22 crevice corrosion to initiate and propagate, three requirements must be present: (i) tight crevices that allow the fast concentration of metal chlorides as well as water of enough ionic strength, (ii) feasible chemistry (high chloride-to-inhibitor concentration ratio) in the bulk environment that can be concentrated even more in the crevice, and (iii) a high enough corrosion potential. In the potential repository setting, the extent of crevice corrosion propagation of Alloy 22 by coupling to Titanium Grade 7 may be limited by the available Alloy 22-to-Titanium Grade 7 crevice area and the probability of the formation of concentrated solutions on the waste package capable of supporting the initiation and propagation of crevice corrosion.

CONCLUSIONS

Crevice corrosion is considered possible if the corrosion potential (E_{corr}) exceeds the repassivation potential for crevice corrosion (E_{rcrev}) in a limited range of environmental and metallurgical conditions. The crevice corrosion susceptibility increased with the increasing chloride concentration, temperature, and increasing chloride to nitrate concentration ratios. Fabrication processes such as welding plus solution annealing also increased the localized corrosion susceptibility of Alloy 22. The crevice corrosion susceptibility appears to be not enhanced by forming similar or dissimilar metal crevices.

Galvanically coupled specimens were used to investigate crevice corrosion propagation in 5 M NaCl at 95 °C [203 °F] under open circuit conditions. The crevice specimens were coupled to either an Alloy 22 or a Titanium Grade 7 plate. Compared to Alloy 22, Titanium Grade 7 appeared to be a more efficient cathode than Alloy 22 resulting in faster crevice corrosion propagation of Alloy 22.

ACKNOWLEDGMENTS

The authors gratefully acknowledge Brian Derby for laboratory assistance, the technical review of O. Pensado, the editorial review of L. Mulverhill, the programmatic review of S. Mohanty and K. Axler, and the assistance of S. Odam in preparing this paper. This paper describes work performed by the Center for Nuclear Waste Regulatory Analyses (CNWRA) for the U.S. Nuclear Regulatory Commission (NRC) under Contract No. NRC–02–02–012. The activities reported here were performed on behalf of the NRC Office of Nuclear Material Safety

and Safeguards, Division of High-Level Waste Repository Safety. This paper is an independent product of the CNWRA and does not necessarily reflect the view or regulatory position of the NRC.

REFERENCES

1. NRC. NUREG–1762, "Risk Insights Baseline Report." Washington, DC: NRC. July 2004.

2. G.A. Cragnolino, D.S. Dunn, C.S. Brossia, V. Jain, and K.S. Chan. "Assessment of Performance Issues Related to Alternate Engineered Barrier System Materials and Design Options." CNWRA 99-003. San Antonio, Texas: CNWRA. 1999.

3. S. Mohanty, T.J. McCartin, and D. Esh (coordinators). "Total-system Performance Assessment (TPA) Version 4.0 Code: Module Descriptions and User's Guide." San Antonio, Texas: CNWRA. 2002.

4. D.S. Dunn, O. Pensado, Y.-M. Pan, L.T. Yang, and X. He. "Modeling Corrosion Processes for Alloy 22 Waste Packages." Scientific Basis for Nuclear Waste Management XXIX, Ghent, Belgium, September 12–16, 2005. P. Van Isheghem, ed. Symposium Proceedings Vol. 932. Warrendale, Pennsylvania: Materials Research Society. pp. 853–860. 2006.

5. D.S. Dunn, Y.-M. Pan, L. Yang, and G.A. Cragnolino. "Localized Corrosion Susceptibility of Alloy 22 in Chloride Solutions: Part 2—Effect of Fabrication Processes." *Corrosion*. Vol. 62. pp. 3–12. 2006.

6. D.S. Dunn, O. Pensado, Y.-M. Pan, R.T. Pabalan, L. Yang, X. He, and K.T. Chiang. "Passive and Localized Corrosion of Alloy 22—Modeling and Experiments." CNWRA 2005-002. San Antonio, Texas: CNWRA. 2005.

7. D.S. Dunn, Y.-M. Pan, L. Yang, and G.A. Cragnolino. "Localized Corrosion Susceptibility of Alloy 22 in Chloride Solutions: Part 1—Mill-Annealed Condition." *Corrosion*. Vol. 61. pp. 1,078–1,085. 2005.

8. X. He and D.S. Dunn. "Alloy 22 Localized Corrosion Propagation in Chloride-Containing Waters." *Corrosion*. Vol. 63. pp. 145–158. 2007.

9. X. He and D.S. Dunn. "Alloy 22 Localized Corrosion Propagation in Chloride-Containing Waters." CNWRA 2006-001. San Antonio, Texas: CNWRA. 2005.

10. ASTM International. "Metals Test Methods and Analytical Procedures." *ASTM G46–94 (2004): Standard Guide for Examination and Evaluation of Pitting Corrosion. Volume 3.02: Wear and Erosion—Metal Corrosion*. Published on CD-ROM. West Conshohocken, Pennsylvania: ASTM International. 2004.

11. D.S. Dunn, Y.-M. Pan, D. Daruwalla, and A. Csontos. "The Effects of Fabrication Processes on the Mechanical Properties of Waste Packages—Progress Report." CNWRA 2004-03. San Antonio, Texas: CNWRA. 2004.

12. D.S. Dunn, D. Daruwalla, and Y.-M. Pan. "Effect of Fabrication Processes on Material Stability—Characterization and Corrosion." CNWRA 2004-01. San Antonio, Texas: CNWRA. 2003.

13. R.L. Tapping. "Surface Studies of Austenitic Alloys Subjected to Crevice Corrosion in Sea Water." *Corrosion Science*. Vol. 25. pp. 363-376. 1985.

14. Y.H. Kim and G.S. Frankel. "Effect of Noblel Element Alloying on Passivity and Passivity Breakdown on Ni." *Journal of the Electrochemical Society*. Vol. 154. pp. C36-C42. 2007.

15. J.R. Hayes, J.J. Gray, A.W. Szmodis, and C.A. Orme. "Influence of Chromium and Molybdenum on the Corrosion of Nickel-Based Alloys." *Corrosion*. Vol. 62. pp. 491-500. 2006.

16. A.C. Lloyd, D.W. Shoesmith, N.S. McIntyre, and J.J. Noël. "Effects of Temperature and Potential on the Passive Corrosion Properties of Alloys C22 and C276." *Journal of the Electrochemical Society*. Vol. 150. pp. B120-130. 2003.

17. A.C. Lloyd, J.J. Noël, S. McIntyre, D.W. Shoesmith. "Cr, Mo and W alloying additions in Ni and their effect on passivity." *Electrochimica Acta*. Vol. 49. pp. 3015-3027. 2004.

18. D.D. Macdonald. "The Point Defect Model for the Passive State." *Journal of the Electrochemical Society*. Vol. 139. pp. 3434-3448. 1992.

19. B.A. Kehler, G.O. Ilevbare, and J.R. Scully. "Crevice Corrosion Stabilization and Repassivation Behavior of Alloy 625 and Alloy 22." *Corrosion*. Vol. 57. pp. 1,042–1,065. 2001.

20. N. Sridhar, D.S. Dunn, C.S. Brossia, and G.A. Cragnolino. "Stabilization and Repassivation of Localized Corrosion." Proceedings of the CORROSION/2001 Research Topical Symposium. G.S. Frankel and J.P. Scully, eds. Houston, Texas: NACE. 2001.

Table 1. Chemical Composition of Engineered Barrier Materials (in Weight Percent)

Material	Ni*	Cr*	Mo*	W*	Fe*	Co*	Si*	Mn*	V*	P*	S*	C*
Alloy 22 Heat 2277-3-3266	Bal	21.4	13.3	2.81	3.75	1.19	0.03	0.23	0.14	0	0	0
Alloy 22 Heat 2277-3-3292	Bal	21.22	13.64	2.96	3.69	1.32	0.02	0.23	0.13	0	0	0
Alloy 622 weld filler wire WN813	Bal	22.24	13.7	3.13	2.37	0.41	0.02	0.34	0	0	0	0
Alloy 22 Heat 2277-1-3133	Bal	21.44	13.27	2.85	4.76	0.65	0.22	0.15	0	0.01	0	0
	Ti*	Pd*	Fe*	C*	N*	O*	H*					
Titanium Grade 7 Heat CN 2775	Bal	0.16	0.08	0	0	0.13	0					

*Ni—nickel, Cr—chromium, Mo—molybdenum, W—tungsten, Fe—iron, Co—cobalt, Si—silicon, Mn—manganese, V—vanadium, P—phosphorus, S—sulfur, C—carbon, Ti—titanium, Pd—palladium, C—carbon, N—Nitrogen, O—oxygen, H—hydrogen.

Table 2. Chemical Composition from Energy Dispersive Spectroscopy Analysis at Locations A and B in Figure 6 (in Weight Percent)

Location	Cl*	Cr*	Mo*	W*	Fe*	Co*	Ni*
A	Not detectable	23.16	13.83	2.71	3.75	1.14	55.41
B	6.6	14.91	62.46	14.97	Not detectable	Not detectable	1.06

*Cl—chloride, Cr—chromium, Mo—molybdenum, W—tungsten, Fe—iron, Co—cobalt, Ni—nickel.

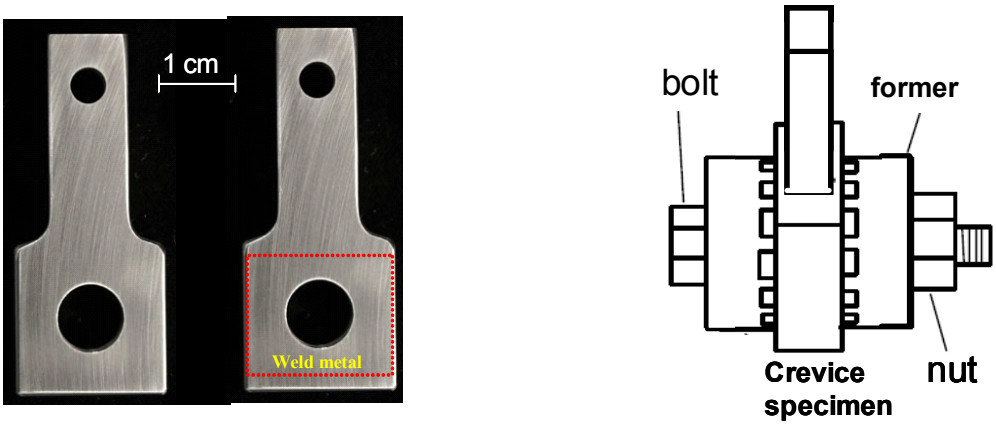

(a) Alloy 22 crevice specimen including mill-annealed and welded plus solution annealed and the crevice assembly as the working electrode

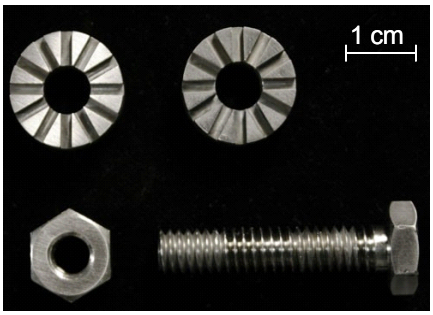

(b) Titanium Grade 7 formers, bolt, and nut

Figure 1. (a) Optical Photos of crevice specimen and illustration of the crevice assembly as the working electrode and (b) optical photos of the metal crevice formers and the fixtures (bolts and nuts) used to assemble crevices

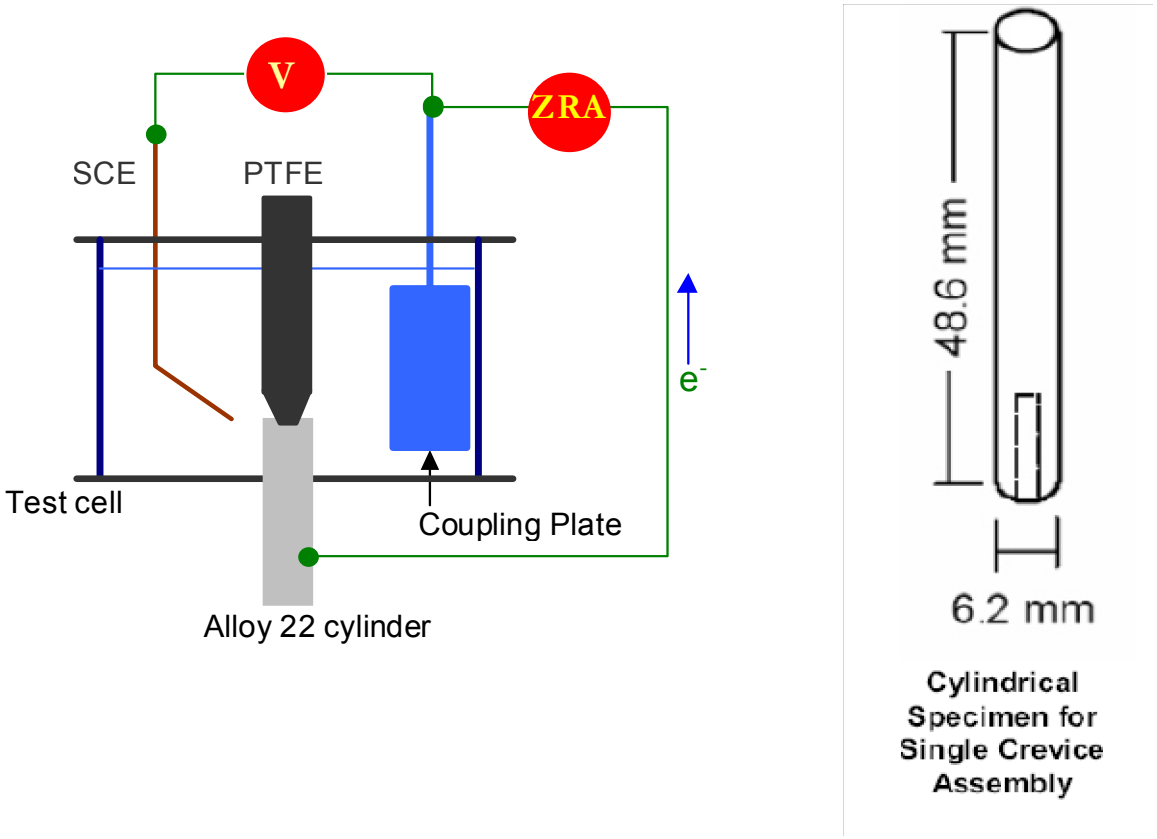

Figure 2. Schematics of the galvanic coupling test cell and the cylindrical specimen. The gas bubbler and thermometer are omitted for clarity.
Note: PTFE = polytetrafluoroethylene; ZRA = Zero resistance ammeter; V = Voltmeter; SCE = saturated calomel electrode.

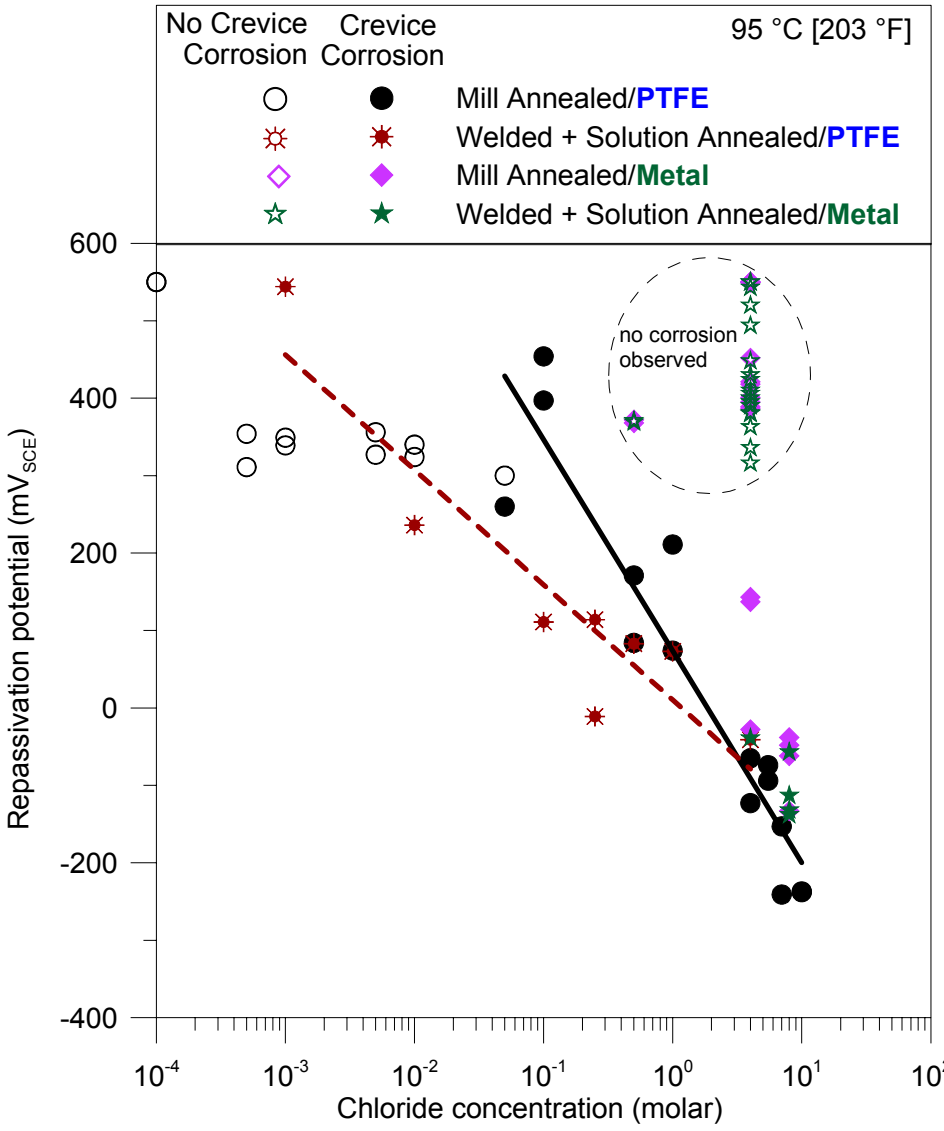

Figure 3. Crevice corrosion repassivation potentials for mill-annealed and welded plus solution annealed Alloy 22 in chloride solutions at 95 °C [203 °F] using polytetrafluoroethylene or metal (Alloy 22 or Titanium Grade 7) as crevice-forming material. The lines are log-linear regression lines of the repassivation potential with chloride concentration.
Note: PTFE = polytetrafluoroethylene

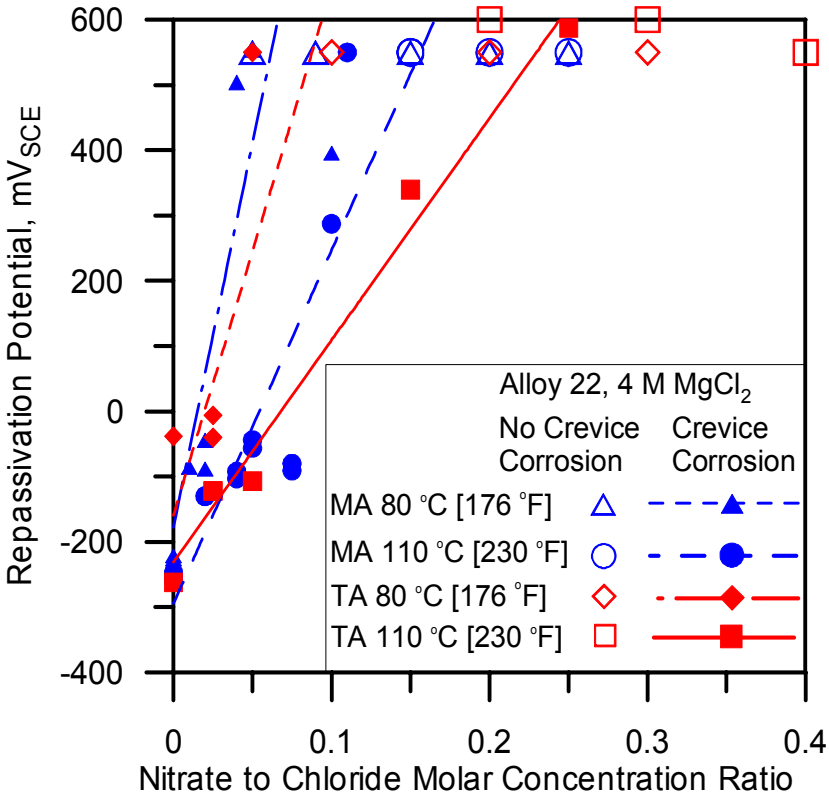

Figure 4. Crevice corrosion repassivation potentials for mill-annealed and thermally aged Alloy 22 in chloride solutions at 80 and 110 °C [176 and 230 °F]. The lines are linear regression lines of the repassivation potential with chloride concentration.

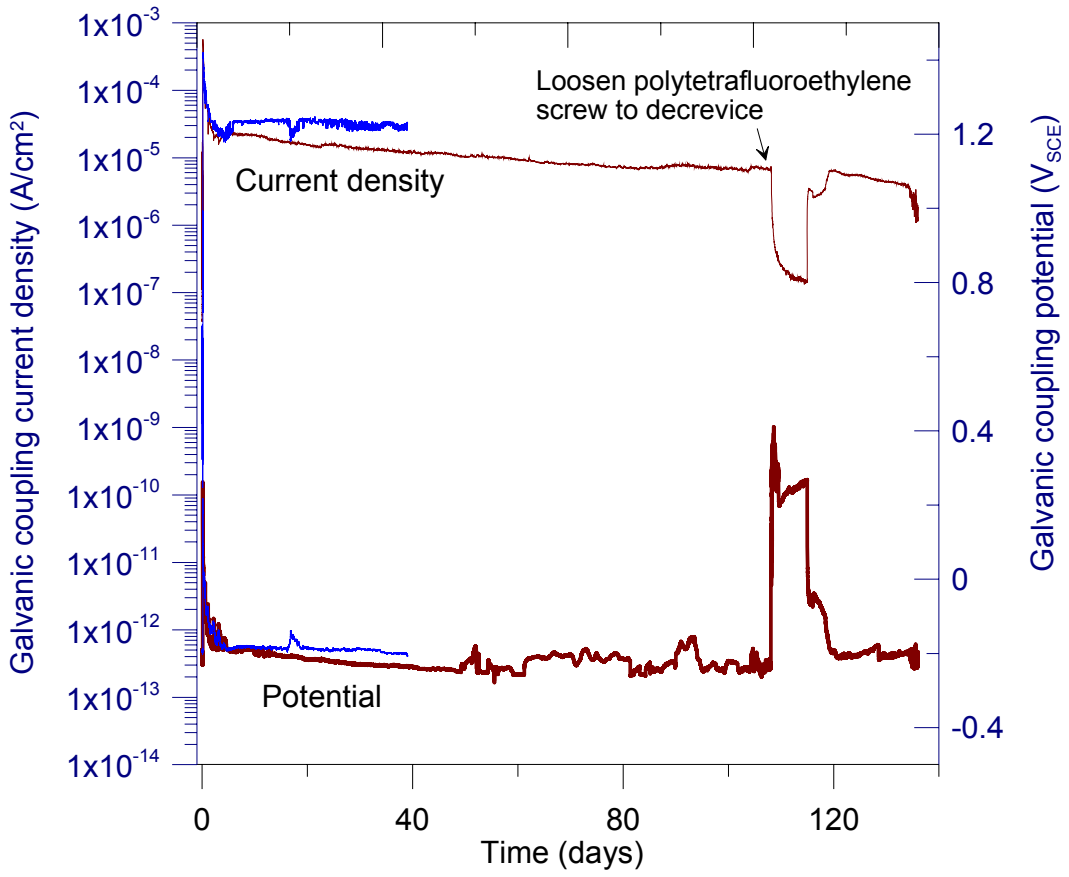

Figure 5. Measured current density and potential for Alloy 22 cylindrical specimen coupled to Titanium Grade 7 in 5 M NaCl plus 2 × 10^{-4} M $CuCl_2$ Solution at 95 °C [203 °F]. The current density is the measured current divided by the entire specimen area exposed to the solution.

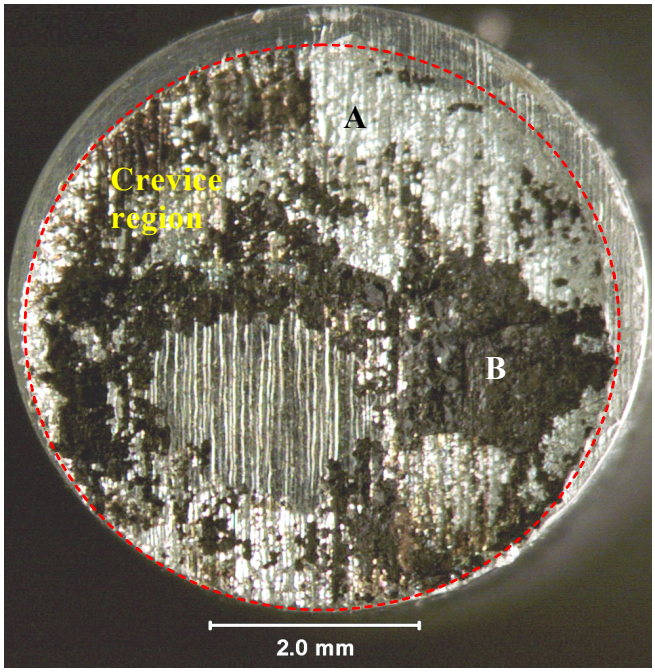

Figure 6. Optical photograph of Alloy 22 crevice specimen after crevice corrosion tests in 5 M NaCl plus 2 × 10^{-4} M $CuCl_2$ solution at 95 °C [203 °F]. The region in the circle is the crevice region. The maximum penetration depth was 460 μm [18.1 mils].

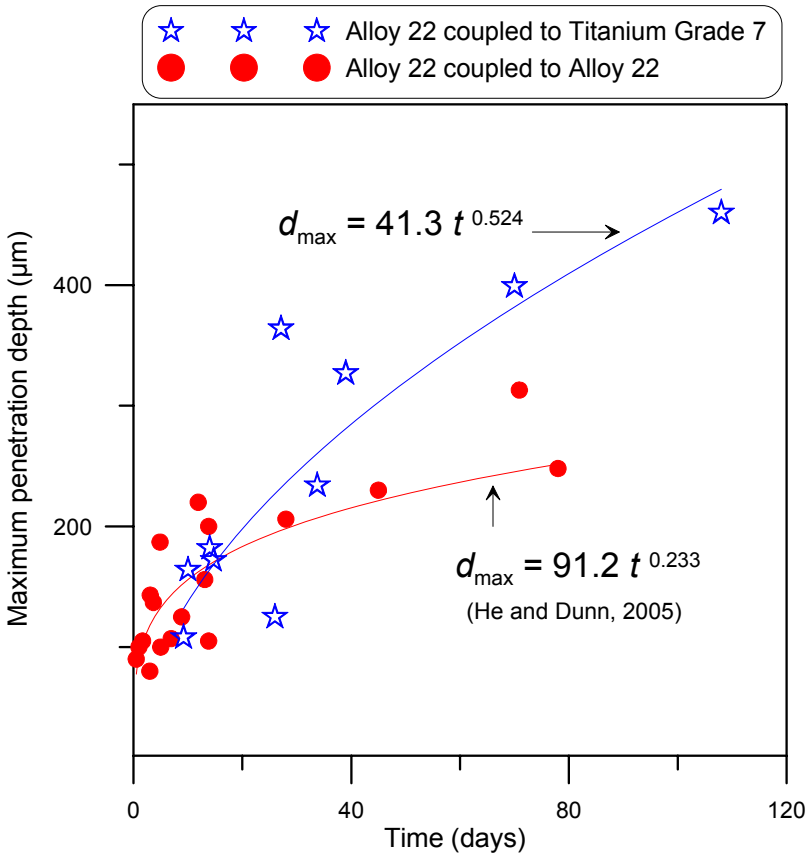

Figure 7. Measured crevice corrosion penetration depths as a function of time for tests on Alloy 22 coupled to Titanium Grade 7 at 95 °C [203 °F] in 5 M NaCl Plus 2 × 10^{-4} M $CuCl_2$ solution along with the other data values from tests on Alloy 22 coupled to Alloy 22 (He and Dunn, 2007, 2005).

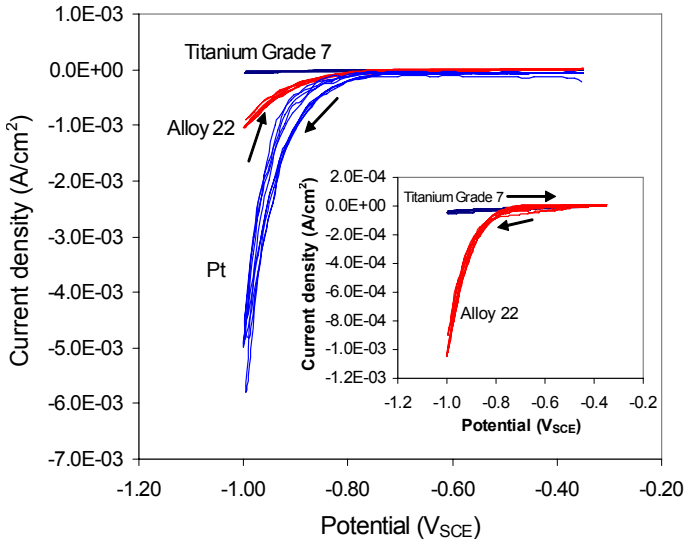

(a)

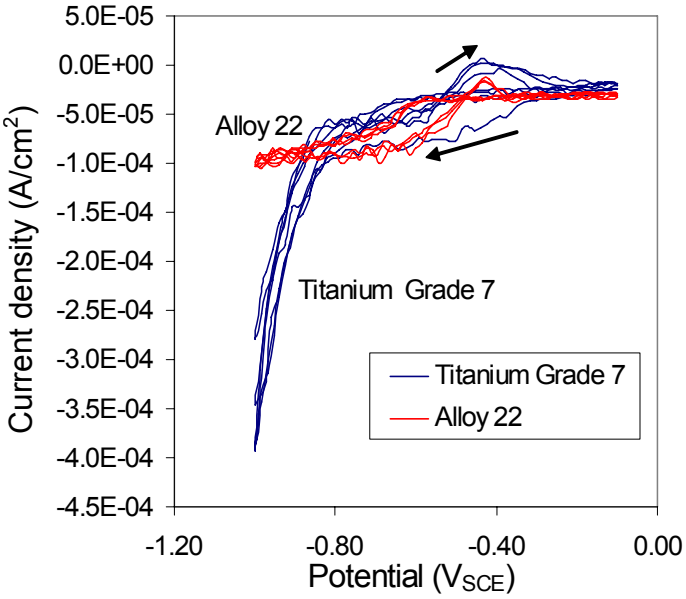

(b)

Figure 8. Cathodic polarization scans performed on (a) Alloy 22, Titanium Grade 7, and Platinum from −0.35 V_{SCE} to −1 V_{SCE} and backward at a scan rate of 5 mV/sec in aerated 5 M NaCl solution and (b) Alloy 22 and Titanium Grade 7 from −0.10 V_{SCE} to −1 V_{SCE} and backward at a scan rate of 5 mV/sec in aerated 5 M NaCl plus 2×10^{-4} M $CuCl_2$ solution.